

1 **Combining hydrologic simulations and stream-network**  
2 **models to reveal flow-ecology relationships in a large**  
3 **Alpine catchment**

4

5 *Stefano Larsen<sup>1,2</sup>; Bruno Majone<sup>2</sup>; Patrick Zulian<sup>2</sup>; Elisa Stella<sup>3</sup>; Alberto Bellin<sup>2</sup>; Maria*  
6 *Cristina Bruno<sup>1</sup>; Guido Zolezzi<sup>2</sup>.*

7

8 1 Fondazione Edmund Mach, Research and Innovation Centre, via E. Mach 1, 38010 San Michele all'Adige,  
9 Italy.

10

11 2 Department of Civil, Environmental and Mechanical Engineering, University of Trento, via Mesiano 77,  
12 38123 Trento, Italy.

13

14 3 Institute of Polar Sciences - Consiglio Nazionale delle Ricerche, Via Torino, 155, 30172, Mestre-Venice,  
15 Italy.

16

17

18

19

20

21

22

23

24

25

26

27

28

29

30

31 **Key points**

32

33

34 The hydrological model HYPERstreamHS was used to simulate natural streamflow series in  
35 100 bio-assessment sites across a large Alpine basin.

36

37 Three flow-regime classes were identified, representing typical nivo-glacial, nivo-pluvial, and  
38 pluvial streams.

39

40

41 Spatial stream-network models identified distinct flow-ecology relationships and **relevant**  
42 **spatial autocorrelation** across classified regimes, which **aid implementing** targeted water  
43 management schemes.

44

45

46

47

48

49

50

51

52

53

54

55

56

57

58

59

60

61

62

63

## 64 **Abstract**

65

66 Flow regimes profoundly influence river organisms and ecosystem functions, but regulatory  
67 approaches often lack the scientific basis to support sustainable water allocation. In part, this  
68 reflects the challenge of understanding the ecological effects of flow variability over different  
69 temporal and spatial domains.

70

71 Here, we use a process-based distributed hydrological model to simulate 23 years of natural  
72 flow regime in 100 target bioassessment sites across the Adige River network (NE Italy), and  
73 to identify typical nivo-glacial, nivo-pluvial, and pluvial reaches. We then applied spatial  
74 stream-network models (SSN) to investigate the relationships between hydrologic and  
75 macroinvertebrate metrics while accounting for network spatial autocorrelation and local  
76 habitat conditions.

77

78 Macroinvertebrate metrics correlated most strongly with maximum, minimum and temporal  
79 variation in streamflow, but effects varied across flow regime types. For example:

80 i) taxon richness appeared limited by high summer flows and high winter flows in nivo-  
81 glacial and pluvial streams, respectively; ii) invertebrate grazers increased proportionally

82 with the annual coefficient of flow variation in nivo-glacial streams but tended to decline  
83 with flow variation in pluvial streams. SSN models revealed that most variation in

84 macroinvertebrate metrics was accounted for by spatial autocorrelation, although local land-  
85 use and water quality also affected benthic invertebrate communities, particularly at lower  
86 elevations.

87

88 These findings highlight the importance of developing environmental flow management  
89 policies in ways that reflect specific hydro-ecological and land use contexts. Our analyses  
90 also illustrate the importance of spatially-explicit approaches that account for auto-correlation  
91 when quantifying flow-ecology relationships.

92

93

94 *Keywords: flow-regime classification; flow-ecology relationships; river networks; benthic*  
95 *invertebrates; network spatial patterns; HYPERstreamHS hydrological model.*

96

97

## 98 **1. Introduction**

99

100 The flow regime of streams and rivers has been modified by human activities at the global  
101 scale (Grill et al., 2019; Tonkin et al., 2019). As human population continues to grow, the  
102 increasing demand for water supply, flood protection and energy production has prompted  
103 the widespread adoption of engineering solutions such as the construction of dams, levees  
104 and other hydraulic infrastructures (Couto & Olden, 2018; Shumilova et al., 2018; Zarfl et al.,  
105 2015). As a result, streams and rivers are under increasing anthropogenic pressure and are  
106 among the most threatened ecosystems worldwide, with particularly high rates of species  
107 extinctions (Tickner et al., 2020). The ongoing global climate change is expected to further  
108 exacerbate this situation by increasing the frequency of extreme hydrologic events such as  
109 floods and droughts that act synergistically with other stressors affecting aquatic ecosystems  
110 (e.g. Navarro-Ortega et al., 2015). This is of particular concern since freshwater ecosystems  
111 support about 10% of all known species (Strayer & Dudgeon, 2010) and are essential for  
112 human well-being, providing a wealth of ecosystem services (Green et al., 2015).

113 Understanding and limiting the ecological effects of flow alteration is therefore fundamental  
114 for a sustainable use of water resources.

115 The Natural Flow Regime Paradigm (Poff et al. 1997) is at the heart of environmental flow  
116 definition and specifically acknowledges that river biota [are](#) adapted to seasonal and  
117 interannual variations of river flow. In order to mitigate the ecological impacts associated  
118 with human infrastructures while maintaining their functioning, environmental flows (termed  
119 *e-flows* hereafter) should mimic the natural streamflow variability in terms of magnitude,  
120 frequency, duration, timing and rate of change (Arthington et al., 2018). However, given the  
121 limits in [the ability to mimic natural regimes in regulated rivers](#), *e-flows* policy must be  
122 informed by a clear understanding of the relation between river ecology and flow  
123 characteristics (i.e., flow-ecology relationships), which is, however, hampered by several  
124 practical challenges. These include, among others: i) the paucity of stream and river locations  
125 for which ecological information can be paired with long term hydrologic records (e.g.  
126 Patrick & Yuan, 2017a); ii) the natural variation in flow regime among rivers and sub-

127 catchments, whereby ecological responses could vary significantly among individual flow  
128 regime types (Poff et al., 2010); and iii) the spatial configuration of river ecosystems, which  
129 requires statistical approaches able to account for the complex autocorrelation associated with  
130 network topology and flow directionality (Peterson et al., 2013).

131

132 Several approaches have been used to address these challenges. Matching flow and  
133 ecological data is a prerequisite for quantifying flow-ecology relationships, and yet the spatial  
134 and temporal overlap between observed hydrologic and biological data is often poor (e.g.  
135 Mazor et al., 2018). To mitigate such limitations, either statistical or process-based  
136 hydrological models have been used. Statistical [hydrological](#) models aim to predict flow  
137 metrics at ungauged locations from the observed relation between available streamflow series  
138 and catchment characteristics (Booker et al., 2015; Patrick & Yuan, 2017b), or by means of  
139 geostatistical interpolation (Skøien et al., 2006). Process-based hydrologic models, on the  
140 other hand, directly simulate streamflow time series at specific network locations by  
141 integrating the hydrological processes acting within the drainage area: i.e., precipitation,  
142 snowmelt, interception, evapotranspiration, infiltration, surface and sub-surface flow, as well  
143 as their interactions (see e.g., Beven, 2012).

144 The second challenge is related to the heterogeneity of river basins where the natural  
145 streamflow regime and river biota differ markedly across the network. Therefore, it is  
146 necessary to classify flow regimes into distinct and easily interpretable classes in order to  
147 define reference flow conditions and implement targeted *e-flows* schemes, while also  
148 minimising the effects of other co-varying environmental factors (Belmar et al., 2011; Booker  
149 et al., 2015). As a result, *e-flows* can be transferred among similar flow regimes at regional  
150 scales. For instance, the identification and classification of reference hydrographs are two key  
151 steps (i.e., “Hydrological foundation” and “River classification”) in the assessment of the  
152 “Ecological Limits of Hydrologic Alteration” (ELOHA), the holistic framework increasingly  
153 adopted to define regional flow standards (Poff et al., 2010).

154 The third challenge is not strictly associated with flow-ecology research, but it is related to  
155 the spatial structure of river networks. The topology of branching river networks implies that  
156 classical statistical methods are unable to account for the spatial autocorrelation due to the  
157 connectivity and directionality of water flow within the network. Failing to account for such  
158 spatial patterns may lead to spurious correlations (Isaak et al., 2014). However, recent  
159 advances in the field of fluvial variography (i.e. spatial statistics applied to river networks)  
160 have provided the tools to model these spatial dependencies over the Euclidean and

161 watercourse dimension, while also accounting for flow directionality (Carrara et al., 2012;  
162 Ver Hoef & Peterson, 2010; Zimmerman & Ver Hoef, 2017). Such stream-network models  
163 have been used to derive spatially-explicit estimates of water quality and population  
164 abundance across river basins (Isaak et al., 2017; McGuire et al., 2014), but applications to  
165 flow-ecology research are surprisingly scarce (Bruckerhoff et al., 2019).  
166 In this paper we develop and discuss a framework that addresses these challenges using the  
167 Adige River basin (northeastern Italy) as case study. In doing so, we aim to contribute to the  
168 understanding of flow-ecology relationships at the regional scale and evaluate potential flow-  
169 sensitive indicators, since recent works in the Italian Alps showed the poor sensitivity of  
170 some of the current Water Framework Directive (WFD) biological indicators to flow  
171 parameters (Larsen et al., 2019; Quadroni et al., 2017). Specifically, we focused on benthic  
172 macroinvertebrates as model organisms because of their essential role in the functioning of  
173 lotic systems, their widespread use as biological indicators and the availability of monitoring  
174 data in the region (De Pauw et al., 2006; Friberg, 2014; Larsen et al., 2019). We included  
175 both taxonomic and functional (traits-based) metrics, as these provide independent and  
176 complementary information that could be valid across biogeographic zones (Heino et al.,  
177 2013).  
178 To achieve the above-mentioned goals, first we used the process-based HYPERstreamHS  
179 hydrological model (Avesani et al., 2020) to simulate the natural streamflow series of one-  
180 hundred stream reaches throughout the Adige River basin where biological information was  
181 available. Then, we classified distinct flow regimes representing the natural hydrological  
182 conditions of the streams in the basin. Subsequently, we used spatial stream-network models  
183 (SSN) to correlate the macroinvertebrate taxonomic and functional metrics with the  
184 streamflow characteristics and habitat conditions within each flow regime, while also  
185 accounting for spatial autocorrelation.

186

187

## 188 **2. Data and Methods**

189

### 190 **2.1 Study area**

191 The study area is the Adige River basin, an Alpine catchment in northeastern Italy (Fig. 1),  
192 closed at ‘Vo Destro’ gauging station (drainage area 10600 km<sup>2</sup>). The Adige River is the  
193 second longest Italian river, with the typical natural streamflow regime of the Alpine region

194 showing two seasonal maxima, one occurring in spring-summer due to snow and glacial  
195 melt, and the other in autumn triggered by cyclonic storms (Chiogna et al., 2016; Mallucci et  
196 al., 2019). Recent analyses of historical hydro-climatic trends revealed that the basin is  
197 sensitive to climate change with ongoing reduction of winter snowfall and anticipation of  
198 snow-melting season (Diamantini et al., 2018; Lutz et al., 2016; Mallucci et al., 2019),  
199 which are likely to alter its flow regime by the second half of 21<sup>st</sup> century (Majone et al.,  
200 2016). Such modifications may have relevant [socio-economic consequences](#) in the  
201 catchment, [where more than 80% of licensed withdrawn water is allocated to large](#)  
202 [hydropower plants, and about 6% to agriculture](#) (Bellin et al., 2016; Zolezzi et al., 2009).  
203 [We selected 100 headwater stream reaches \(Fig.1\) throughout the catchment for which](#)  
204 [biological information was available and with an almost pristine streamflow regime \(i.e. no](#)  
205 [major in-stream hydraulic infrastructure or impoundments upstream\)](#). The selected reaches  
206 [were mostly 1<sup>st</sup> and 2<sup>nd</sup> order streams, with elevation and drainage area ranging from 170 to](#)  
207 [1900 m a.s.l. and from 10 to 434 km<sup>2</sup>, respectively.](#)

208

## 209 **2.2 Observational datasets**

### 210 **2.2.1 Flow data**

211 The regional precipitation and temperature dataset ADIGE (Mallucci et al., 2019) was used  
212 as meteorological forcing for hydrological modelling. This dataset provides daily  
213 precipitations and temperatures for the time interval 1956-2013 at the spatial resolution of 1  
214 km. The dataset was developed by interpolating the measurements available at the  
215 meteorological stations within and nearby the river basin by means of kriging with external  
216 drift (Goovaerts, 1997; Mallucci et al., 2019). To comply with the computational grid  
217 adopted in the hydrologic modeling, the ADIGE dataset was aggregated to 5-km grid  
218 spacing.

219 Daily streamflow data collected at 9 gauging stations ([Fig.1](#)) were provided by the  
220 Hydrological Office of the Autonomous Provinces of Trento ([www.floods.it](http://www.floods.it)) and Bolzano  
221 ([www.provincia.bz.it/hydro](http://www.provincia.bz.it/hydro)). Stations were selected according to the following criteria: i)  
222 observational period including the 1989–2013 time-frame used for calibration and validation  
223 of the hydrological model; ii) limited gaps in records; iii) large distance from upstream  
224 reservoirs if present; and, iv) broad spatial coverage including the major tributaries of the  
225 Adige River. The gauging stations were distributed in sub-catchments of different sizes,

226 elevation, geology and land-cover, and were therefore representative of the hydrological  
227 regimes of the Adige basin.

228

### 229 *2.2.2 Macroinvertebrate data*

230 Macroinvertebrate data were collected by the Environmental Protection Agencies of the  
231 Provinces of Trento and Bolzano as part of their institutional monitoring programmes (Larsen  
232 et al., 2019). Sampling was performed according to the multi-habitat sampling approach  
233 defined in the AQEM (<http://www.aqem.de/>) protocol: 10-replicate Surber samples were  
234 collected within a 20-50 m reach in proportion to the micro-habitats present (Hering et al.,  
235 2004). Samples were collected in the period 2009-2015, and sites were visited several times  
236 per year (median = 3), primarily in spring and autumn. Macroinvertebrate densities were  
237 averaged over all samples to remove seasonal effects, thereby obtaining a representative  
238 community composition of each site.

### 239 *2.2.3 Reach-scale environmental data*

240 Two additional reach-scale environmental variables were included in the analyses besides  
241 streamflow regime: the proportion of agricultural land-use (“Agr.landuse”), calculated within  
242 1-km buffer around each sampling location, and the [physico-chemical water quality](#), as  
243 expressed by the “LIMeco” index (Livello di Inquinamento da Macrodescrittori per lo stato  
244 ecologico), one of the official WFD water quality indicators used to assess the ecological  
245 status of running water in Italy (European Commission, 2000). This is a multi-metric  
246 indicator assigning quality scores based on threshold levels for concentration of oxygen,  
247 ammonia, nitrate and total phosphorus in freshwater (see Azzellino et al., 2015). These  
248 environmental descriptors were included as covariates in the quantification of flow-ecology  
249 relationship because of their [proven](#) influence on the composition of benthic invertebrates in  
250 the area (Larsen et al., 2019).

251

252

## 253 *2.3 Hydrologic simulations*

254 Hydrological simulations were performed at the daily time scale with the HYPERstreamHS  
255 model (Avesani et al., 2020; Laiti et al., 2018), which couples the HYPERstream routing  
256 scheme (recently proposed by Piccolroaz et al., 2016) with a continuous Soil Conservation  
257 Service (SCS) module for surface flow generation (Michel et al., 2005). Subsurface return  
258 flow was modelled by a nonlinear reservoir (Majone et al, 2010). [The](#) HYPERstream routing

259 scheme is specifically designed to couple with climate models and, in general, with gridded  
260 meteorological datasets. HYPERstream inherits the computational grid of the climatic model,  
261 or of the gridded product providing the meteorological forcing, and preserves  
262 geomorphological dispersion due to the structure of the river network (Rinaldo et al., 1991),  
263 regardless of grid resolution. In previous studies, the SCS runoff module was successfully  
264 applied to two tributaries of the Adige River (Bellin et al., 2016; Piccolroaz et al., 2015). For  
265 a detailed description of the hydrologic modelling framework see Laiti et al., (2018) and  
266 Avesani et al. (2020).

267 The hydrological model was calibrated against daily streamflow observations in the time  
268 window 1989-2013 using the ADIGE dataset as input meteorological forcing. The parameters  
269 space was explored for optimality, according to the Nash-Sutcliffe efficiency index (NSE;  
270 Nash & Sutcliffe, 1970), by using the Particle Swarming Optimization algorithm (Kennedy &  
271 Eberhart, 1995). NSE was selected because of its effectiveness in assessing the performance  
272 of hydrologic models in reproducing observed streamflows. NSE is satisfactory when larger  
273 than 0.5 (Moriassi et al., 2007). Because hydrologic modelling was tailored to reproduce  
274 streamflow at unimpacted headwater locations (see Sect. Study area), four headwater gauging  
275 stations (Vermiglio, Rio Funes, Aurino and Gadera in Fig.1) were calibrated simultaneously  
276 (i.e. NSE was defined as the average of individual efficiencies from the four stations).  
277 Successively, other five stations distributed across the basin (Saltusio, Vipiteno, Anterselva,  
278 Trento and Bronzolo in Fig.1; drainage area ranging from 60 to 9000 km<sup>2</sup>) were used for  
279 validation, in order to assess how the model reproduced streamflow at all the relevant scales.  
280 The first two years of the time series, i.e., 1989 and 1990, were used as spin-up for the  
281 simulations and therefore were excluded from the computation of NSE. Finally, we used the  
282 calibrated hydrologic model to simulate streamflow time series (1991-2013) at the 100  
283 gauged and ungauged locations where biological data were available.

284 As additional validation of the hydrologic model, we compared patterns of flow-ecology  
285 relationships obtained from the observed and simulated streamflow using nine locations for  
286 which measured streamflow time series were also available.

#### 287 **2.4 Hydrologic classification**

288 Simulated streamflow time series at the 100 locations were first normalised by their mean  
289 annual discharge (MAD) to allow comparison across streams and develop flow-ecology  
290 relationships independent of stream size (e.g. Rosenfeld, 2017). In the following step,

291 streamflow regimes were classified according to their typical seasonality as follows: first, we  
292 calculated the mean monthly hydrographs for each location from the MAD-normalised daily  
293 streamflow time series (Fig. S1 in SM); then we performed a Principal Component Analysis  
294 (PCA) on the resulting hydrographs to synthesize similarities among locations using the first  
295 two PC axes. Location scores on the two axes were then weighted by the proportion of  
296 variance explained in the PCs and used as synthetic variables in order to cluster the locations  
297 based on their flow regime (see e.g. Belmar et al., 2011). A flexible-beta hierarchical  
298 clustering approach was used, with the recommended value of  $\beta = -0.25$  (Belmar et al.,  
299 2011; Legendre & Legendre, 2012; Mazon et al., 2018), which provides an intermediate  
300 solution between chaining obtained via single linkage, and space dilation deriving from  
301 complete linkage. To further validate the degree of separation among the classified regimes,  
302 we ran a Permutational Multivariate Analysis of Variance (PERMANOVA; Anderson, 2017)  
303 based on the Euclidean distance matrix of the weighted PCA scores.

304

## 305 **2.5 Hydrologic metrics**

306 We used the 23 years MAD-normalised daily streamflow values to calculate 34 hydrologic  
307 metrics following the Indicator of Hydrologic Alteration (IHA; Richter et al., 1997) approach  
308 (Tab. 1), implemented in R software with the “IHA” package (R Core Team, 2019). These  
309 metrics were averaged over the years to quantify ecologically-relevant components of the  
310 long-term flow regime related to magnitude, duration, frequency, timing and rate of change.  
311 As an exploratory step, and to visualise and further validate the separation of the hydrologic  
312 classes in the multidimensional space defined by the hydrologic metrics, we plotted the  
313 streams on the first two PCA axes derived from the correlation matrix of the IHA metrics  
314 (Fig. 4). However, our main interest was to quantify flow-ecology relationships within the  
315 distinct hydrologic regimes considered as management units. Therefore, we ran additional  
316 PCA analyses for each classified regime to identify the most relevant metrics in each group.  
317 We then selected a set of non-redundant flow metrics showing high correlation ( $>0.8$ ) with  
318 the 1<sup>st</sup> or 2<sup>nd</sup> PC axes (see Tab. S1 and Results), which reflected the key flow components.  
319 These flow metrics were subsequently used as predictors in stream-network models for  
320 quantifying interpretable flow-ecology relationships.

321

322

## 323 **2.6 Data analysis**

324 We derived a set of taxonomic and functional metrics from the macroinvertebrate community  
325 data. Our aim was to examine the sensitivity of different metrics to streamflow conditions to  
326 derive valid alternatives to those currently implemented under the WFD. We included metrics  
327 related to the diversity of the community, such as taxonomic richness, Shannon diversity (as  
328 effective number of species of order  $q=1$ ; Jost, 2006), Functional Dispersion (FDis, which is  
329 minimally influenced by taxonomic richness), as these have been shown to reflect flow  
330 alterations elsewhere (e.g. Kennedy et al 2016). We additionally included metrics describing  
331 the proportion of different feeding groups (i.e. grazers, shredders, gatherers, filterers and  
332 predators) and the proportion of relatively small and large sized (range 0.25-0.5 mm and 20-  
333 40 mm, respectively) invertebrates. We focused on feeding traits as they convey information  
334 about the functional role of organisms in the ecosystems and on size traits that are a proxy of  
335 multiple life-history characteristics like e.g. life cycle duration, longevity (Poff et al., 2006)  
336 and may respond to variation in shear stress (e.g. Merigoux & Doledec, 2004). Finally, we  
337 also examined how the WFD Star\_ICMi index responded to flow characteristics. The  
338 Star\_ICMi is the official Biological Quality Element used in Italy to classify the status of  
339 running water in line with the WFD requirements (Buffagni et al., 2006; Buffagni & Erba,  
340 2007). The index is formulated combining six normalised and weighted metrics, including  
341 richness, diversity and taxa sensitivity to organic pollution (Buffagni et al., 2006).  
342 Information for functional traits of the taxa was gathered from the online database of  
343 freshwater ecology (www.freshwaterecology.info; Schmidt-Kloiber & Hering, 2015). For the  
344 calculation of FDis, we included 13 traits (Tab. S2) in order to provide an inclusive measure  
345 of functional diversity. Feeding information was available for all taxa included in the  
346 analysis, whereas size traits were available for about 50% of the taxa. As such, taxa with no  
347 information for a given trait, were not considered in the analyses.

348

#### 349 *2.6.1 Spatial stream-network models*

350 Spatial stream-network models (SSN; Ver Hoef et al., 2014; Ver Hoef & Peterson, 2010)  
351 were run separately for each flow regime to quantify the relation between the biotic and  
352 hydrologic metrics, while accounting for the autocorrelation structures of the dendritic  
353 network. The LIMeco index and Agr.landuse indicator were included as additional covariates  
354 in the models. ArcMap 10.5 and the STARS toolset (Peterson & Hoef, 2014) were used to  
355 generate the spatial data necessary to analyse stream-network models. The full set of  
356 autocovariance functions were used to model spatial autocorrelation, including Euclidean, in-  
357 stream flow-connected (locations in which water flows from one to the other) and flow-

358 unconnected (connected within the network, but not reflecting the directionality of the water  
359 flow) functions. This approach allows accounting simultaneously for the along-channel and  
360 across-basin (flow-unconnected and Euclidean, respectively) patterns of autocorrelation,  
361 while also distinguishing locations linked by direct water flow (i.e. flow-connected). In  
362 particular, SSN models take the form:

363

$$364 \quad y = X\beta + z_{TU} + z_{TD} + z_{EU} + \varepsilon \quad (1)$$

365

366 where  $y$  is the response variable (i.e., macroinvertebrate metrics in this study),  $X$  is the matrix  
367 of predictors (flow metrics, LIMeco, and Agr.landuse) with associated  $\beta$  regression  
368 parameters, while  $z_{TU} + z_{TD} + z_{EU}$  are zero-mean random variables with autocorrelation  
369 structure based on tail-up (TU), tail-down (TD) and Euclidean (EU) functions, respectively,  
370 and  $\varepsilon$  is the random independent error. The TU and TD functions are moving-averages  
371 functions autocorrelated [in an upstream and downstream direction, respectively](#). Tail-up  
372 function assigns different weights to locations upstream of a given site according to the  
373 catchment area, used here as a proxy of streamflow. In this way, the moving-average  
374 autocorrelation is split at confluences so that upstream locations with larger catchments have  
375 a stronger influence on downstream communities. The reader can refer to Peterson et al.  
376 (2013) and Ver Hoef et al. (2010) for a detailed description of the SSN framework.

377

378 Biotic metrics expressed as proportions (i.e. feeding and size traits) were logit-transformed as  
379 recommended (Warton & Hui, 2011), and maximum-likelihood was used for parameter  
380 estimation in all SSN models. For each biotic metric, the most supported model was selected  
381 based on the root mean-square prediction errors (RMSPE), which focus on model predictive  
382 power (Ver Hoef et al. 2014). The model was developed in a stepwise fashion, following  
383 guidelines provided in Ver Hoef et al. (2014). We first included all predictors ([the selected  
384 flow metrics](#), LIMeco, Agr.landuse), and the full set of autocovariance functions (i.e. tail-up,  
385 tail-down and Euclidean). [Then we manually removed non significant predictors and  
386 subsequently refined the spatial components. These can be defined by considering different  
387 autocovariance functions, including e.g. exponential, Mariah, spherical, linear-with sill,  
388 though spatial stream-network models appear little influenced by their mis-specification  
389 \(Garreta et al. 2009; Isaak et al. 2014\). We compared or removed different functions for the  
390 Euclidean, tail-up and tail-down components and selected the final model with the lowest  
391 RMSPE. If different models had identical RMPSE values, the most parsimonious solution](#)

392 was selected based on Akaike Information Criterion (AIC). The spatial autocovariance  
393 functions were refined after the selection of the model predictors, since the model accounts  
394 for spatial correlation in the error term after the effects of the covariates is removed (Frieden  
395 et al. 2014).

396

397 The SSN package (Ver Hoef et al. 2014) for R software (R Core Team, 2019) was used to run  
398 the stream-network models.

399

400

### 401 **3. Results**

402

#### 403 ***3.1 Hydrologic simulations and classification***

404 The capability of HYPERstreamHS hydrological model to reproduce the observed daily  
405 streamflow time series in the Adige River was validated in the period 1991- 2013 by  
406 computing NSE at the 9 gauging stations described in Sect. 2.4 (Fig. 1). The parameters of  
407 the hydrologic model were inferred by maximizing the average NSE at Vermiglio, Rio Funes,  
408 Aurino and Gadera gauging stations. Calibration produced a satisfactory mean NSE of 0.623  
409 (range: 0.58-0.70; Figs. S2 and S3). At the validation stations, mean NSE was 0.620 (range:  
410 0.48-0.79), with lower values in the smaller subcatchments (Saltusio, Isarco, Anterselva; Fig.  
411 S2), and higher values at the larger downstream subcatchments of Trento and Bronzolo (0.74  
412 and 0.79, respectively; Figs. S2 and S3). Remarkably, average value and range of variation of  
413 NSE efficiency did not deteriorate from calibration to validation sites, suggesting that the  
414 model parameters are representative of the entire river basin. The limited reduction of NSE  
415 efficiency at Saltusio, Vipiteno, and Anterselva gauging stations is in line with the general  
416 understanding that an accurate reproduction of observed streamflows in small catchments  
417 would require accurate and spatially well-resolved precipitation and temperature fields at  
418 small spatial scales (e.g., Heistermann & Kneis, 2011). A further validation of the hydrologic  
419 model emerged from the consistent relationship between taxon richness and the IHA flow  
420 metrics across observed and simulated flow data, for the locations where measured  
421 streamflow series were available (Fig. S4).

422 The calibrated model was subsequently used to simulate flow time series for the period 1991-  
423 2013 in the 100 reference locations for which biological data were available, and to perform  
424 the flow regime classification. Three hydrologic classes with distinct flow regimes were

425 identified by the flexible beta-clustering of the first two weighted PC scores (explaining 92%  
426 of the variation) derived from the scaled monthly hydrographs (Fig. 2). The first hierarchical  
427 division separated typical “pluvial” streams (n=38), with peak flow in autumn, from those  
428 with spring and summer peaks. The second division further distinguished streams with “nivo-  
429 glacial” regime (n=30) with summer peak flows and winter low flows, from intermediate  
430 “nivo-pluvial” streams (n=32), with earlier spring peak flows and relatively higher autumn  
431 flows. A PERMANOVA based on Euclidean distances further validated the separation  
432 among the three groups with  $R^2 = 0.85$ . Fig. 1 shows the distribution of the flow regime  
433 classes in the Adige River network. The three flow regimes were distributed along an  
434 altitudinal gradient, which reflects also the gradient of anthropogenic influence in the  
435 catchment (Fig. 3). Indeed, pluvial streams at lower altitude were characterised by more  
436 eutrophic (higher LIMeco scores) waters and higher proportion of agricultural land-use in the  
437 adjacent area.

438

439 The three hydrologic classes identified in the previous step formed three groups in the first  
440 PCA factorial plane (i.e., the first two PCs) derived from IHA metrics, explaining about 80%  
441 of the total variation (Fig. 4). This analysis provided additional evidence of the separation  
442 among the flow regimes, and allowed identifying the metrics that differed the most among  
443 them. For instance, as also evident from the annual hydrographs shown in Fig. 2, nivo-glacial  
444 streams displayed higher flow maxima during summer months (June, July; Figs. 4 and S5) as  
445 well as faster fall and rise rates. Conversely, streams with pluvial regime showed higher flow  
446 minima (e.g. 30 Day Min) and Base index, but more frequent low flow events (Fig. S5).  
447 Nivo-pluvial streams systematically showed flow metrics that were intermediate between the  
448 nivo-glacial and pluvial regimes.

449 The first two PCA axes extracted separately within each flow regime, accounted for 75%,  
450 81% and 76% of variation in IHA metrics across the nivo-glacial, nivo-pluvial and pluvial  
451 regime, respectively. The loadings of the IHA metrics on the PC axes are shown in Tab. S1,  
452 and were used for a parsimonious selection of non-redundant flow metrics to include in the  
453 SSN models. After removing correlated metrics, the selection included: February and July  
454 streamflow, Low pulse number, Fall rate and annual CV (y.CV). These metrics are included  
455 in the first, fourth and fifth flow components of the IHA classification, respectively (Tab.1).  
456 However, February and July flow magnitude were strongly correlated with minimum and  
457 maximum flows as well as with the Base index, and thus represented a proxy for the second  
458 flow component of the IHA classification, which is related to the magnitude of extreme

459 events. Metrics describing the timing of extreme flows (third component) were not included  
460 as they were not particularly relevant within each flow regime, but rather differed among  
461 regimes.

462

### 463 **3.2 Flow-ecology relationship**

464 A total of 64 invertebrate taxa were identified, mostly at family and genus level (see Tab.  
465 S3). The SSN models identified several significant relationships between biotic and  
466 hydrologic metrics and the covariates related to water quality and land-use (Fig. 5; Tab. S4).  
467 The relations differed among the flow regimes both in terms of explained variance and  
468 selected covariates. Overall, the influence of water quality (LIMEco index) and agricultural  
469 land-use on macroinvertebrate communities was also evident, especially for pluvial streams  
470 at lower altitude.

471 Few response variables responded consistently to the hydrologic metrics across flow regimes,  
472 and rather, flow-ecology relationships often displayed divergent patterns (Fig. 6). For  
473 instance, while taxon richness declined significantly with February flow magnitude in pluvial  
474 streams, it tended to increase in the nivo-glacial streams, where instead it declined  
475 significantly with increasing July flow. Similarly, while Shannon diversity increased with the  
476 LIMEco index consistently across flow regimes, it showed a positive association with the  
477 number of low pulses, but only in the pluvial streams. Trait-based metrics also displayed  
478 rather unique patterns for each flow regime. The proportion of grazers displayed different  
479 relations with February flows across the three regimes. In addition, grazers increased  
480 significantly with annual flow variation (y.CV) only in nivo-glacial streams, while the  
481 proportion of filter feeders declined with increasing February flow, but only in the pluvial  
482 streams (Fig. 6).

483 Overall, spatial autocorrelation, considering the flow-connected, flow-unconnected and  
484 Euclidean dimensions (i.e.  $z_{TU}$ ,  $z_{TD}$ ,  $z_{EU}$  in equation 1), explained a larger proportion of  
485 variance (respectively 50%, 77% and 44% in the nivo-glacial, nivo-pluvial and pluvial  
486 streams) than the model predictors ( $X\beta$  in equation 1), which explained 13-26% of the  
487 variance (Fig. 7). The tail-up and tail-down components (reflecting autocorrelation along the  
488 watercourse dimension) explained more residual variance (mean across flow regime: 35.3%)  
489 than the Euclidean spatial component (mean: 21.5%).

490

491

492

#### 493 4. Discussion

494

495 In this study we developed and applied a framework to assess the relationship between river  
496 ecology and flow characteristics, while overcoming some of the challenges typically  
497 associated with flow-ecology research. By employing the HYPERStreamHS hydrological  
498 model, we were able to reproduce natural streamflow time series at 100 ungauged biological  
499 sampling stations throughout the Adige River basin. An important validation of the model  
500 stems from the consistent patterns of flow-ecology relationships obtained from the observed  
501 and simulated streamflow. This is key when hydrological models are used to investigate  
502 ecological responses (Kiesel et al., 2020), as the uncertainty associated with modelled  
503 streamflow is a fundamental limitation hampering the study of flow-ecology relationship at  
504 the pan-European scale (Vigiak et al., 2018). We subsequently identified three distinct flow  
505 regime classes within which flow-ecology relationships were examined using spatially-  
506 explicit geostatistical approaches. This allowed us to account for the natural variability of  
507 flow regimes, while also controlling for the spatial autocorrelation patterns of dendritic river  
508 networks.

509 The three identified flow regimes represent typical hydrologic patterns of the Alpine region.  
510 Low-order streams at higher elevation are fed primarily by glacial melt, snowmelt and  
511 associated groundwater flow; streams at intermediate elevations by snowmelt and rain, and  
512 those at lower elevation mirror rainfall timing. While realistically representing a gradient of  
513 conditions, the three regimes were distinct enough to form separate groups according to both  
514 mean annual flow series and flow metrics. As such, they showed distinct flow-ecology  
515 relationships, especially dependent on high and low streamflow conditions and interannual  
516 variability in discharge.

517 The three flow regimes were also well-separated along a gradient of anthropogenic influence  
518 represented by water quality and riparian land-use. This further highlights how classifying  
519 regimes can help minimise the effect of confounding factors in flow-ecology research: as  
520 streams with different flow regimes often occupy separate sections of the catchment,  
521 systematic difference in elevation, anthropogenic land-use and underlying geology may  
522 confound the influence of streamflow characteristics, hindering the robust identification of  
523 flow-ecology relationships.

524 Surprisingly, while the classification of flow regimes is a common endeavour in hydrologic  
525 research (e.g. Belmar et al., 2011; Di Prinzio et al. 2011; McManamay et al., 2012; Snelder &  
526 Booker, 2013), its applications in flow-ecology studies remains relatively rare.

527 The few studies that have compared flow-ecology relations across classified flow regimes  
528 (e.g. Bruckerhoff et al., 2019; Mims & Olden, 2012), indeed showed that ecological  
529 responses can often diverge. The three streamflow typology analyzed here, in fact, are  
530 characterized by different levels of environmental harshness, which declines with decreasing  
531 glacial influence (Brighenti et al 2020). Had we combined all streams in the same analysis,  
532 we would have drawn different conclusions regarding the response of some biotic metrics,  
533 such as taxon richness and the proportion of grazers (*cfr* grey dashed line with individual fits  
534 in Fig. 6). Richness, for instance, appeared limited by different flow characteristics; it  
535 declined with increasing July flows in the nivo-glacial streams (representing the summer peak  
536 of snow- and glacial-melt), while in the pluvial regime, richness declined with increasing  
537 February flows (representing the winter low rainfall periods). Summer discharge is high in  
538 nivo-glacial streams, where increasing flows could cause higher drift rates and thus lower the  
539 observed benthic richness (e.g. Brittain & Eikeland, 1988, Naman e al., 2015). It is known  
540 that in glacial-fed streams at high elevation, invertebrate abundances can be greatly reduced  
541 in summer due to the increased environmental harshness (Robinson et al., 2004; Ilg et al.,  
542 2001). Conversely, in temperate streams characterized by pluvial regimes, minimum densities  
543 often occur in winter (Brittain & Eikland, 1988), when higher-than-average flows could  
544 further decrease benthic richness. In the nivo-pluvial and pluvial streams, in fact, the  
545 magnitude of February flows appeared to limit the biotic metrics mainly related to  
546 community diversity (i.e. richness, Star\_ICMi, Fdis). On the other hand, the number of low  
547 flow pulses displayed mainly positive association with both diversity and trait based metrics  
548 across flow regimes. Low flow pulses can increase local diversity by preventing excessive  
549 drift while also favoring the deposition of fine organic matter, as suggested by the positive  
550 response of gatherers. Together with the positive association of both grazers and gatherers  
551 with the annual coefficient of variation in nivo-glacial streams, these results indicate how  
552 natural flow variation is fundamental for sustaining aquatic biodiversity.

553

554 The SSN models revealed how the STAR\_ICMi index mostly responded to streams' physico-  
555 chemical parameters and riparian land-use. In agreement with recent investigations (Larsen et  
556 al., 2019; Quadroni et al., 2017), these results provide additional evidence of the limited  
557 sensitivity of WFD biological quality indicators, such as the Star\_ICMi index, to stream

558 hydrologic conditions. As most present bioindicators (Friberg, 2014), the Star\_ICMi is  
559 designed to reflect organic pollution and habitat degradation, and should be used for  
560 hydrologic assessment or guide *e-flows* with great caution. Indeed, one of the aims of the  
561 present study was to evaluate alternative metrics that could serve as flow-sensitive indicators  
562 to be included in assessment schemes like the one of the European WFD. To this end, species  
563 life-history traits can provide the mechanistic link between river biota and flow conditions  
564 that could be valid across large spatial scales (Heino et al., 2013; Mims & Olden, 2012). In  
565 the Adige River basin, the relative proportion of different feeding habits and body size  
566 structure appeared relatively sensitive to hydrologic conditions across flow regimes and thus  
567 deserve further investigation. The sensitivity of grazers to flow conditions, for example, can  
568 derive from their reliance on attached algae, which can be scoured during high flows or  
569 buried by fines during low flows (Buchanan et al., 2013; Doretto et al., 2020; Kennen et al.,  
570 2010). Nonetheless, our results suggest that their response to flow conditions can differ  
571 substantially across flow regimes. The response of body size structure to the magnitude of  
572 high and low flows may reflect the sensitivity of different developmental stages to shear  
573 stress, especially for insect larvae (e.g. Merigoux & Doledec, 2004), but detailed information  
574 on body size was not available for many taxa, and this response requires further examination.  
575

576 Overall the SSN modelling revealed rather idiosyncratic responses of the biotic metrics to  
577 flow conditions. On the other hand, the effect of water quality and local land-use appeared  
578 generally consistent with a positive and negative effect of LIMeco and agricultural land-use,  
579 respectively. This has both practical and fundamental implications. From an applied  
580 perspective, it implies that ecological responses to flow alterations can be contingent on local  
581 eco-hydrologic conditions, a caveat which must be considered when setting regional flow  
582 standards. In the Adige Basin, for instance, sustaining invertebrate richness, or specific  
583 feeding groups, would require a distinct management of high and low flows among the  
584 identified flow regimes.

585 On a more fundamental level, it indicates that the often observed nonlinear flow-ecology  
586 relationships (Rosenfeld, 2017) can reflect the distinct response of multiple flow regimes in  
587 the basin. More generally, the “shape” of flow-ecology relationships is likely to be scale-  
588 dependent and determined by the range of hydrologic conditions in the region and the size of  
589 the species pool included.

590

591 The three identified flow regimes formed geographically separated clusters along a north-  
592 south axis, reflecting the orography of the basin. While this further validated our flow regime  
593 classification, it also introduced possible autocorrelation issues. The SSN models revealed  
594 that most variation in macroinvertebrate metrics was in fact associated with spatial patterns.  
595 This is typical for communities [dwelling in](#) complex habitats, such as river networks, whose  
596 geometry and flow directionality influence environmental and [eco-evolutionary](#) dynamics  
597 (Frieden et al., 2014; Isaak et al., 2014; Larsen et al., 2019). [For some biotic metrics, the](#)  
598 [spatial autocorrelation was by far the most important component, explaining more than 80%](#)  
599 [of the variation \(e.g. Shannon diversity and gatherers in both nivo-glacial and nivo-pluvial](#)  
600 [streams\). Not surprisingly, given the dendritic configuration of river networks and the](#)  
601 [directionality of water flow, autocorrelation along the watercourse dimension \(i.e. tail-up and](#)  
602 [tail-down\) appeared stronger than over the isometric Euclidean dimension. However, the](#)  
603 [influence of autocorrelation differed across regimes, being particularly large in the nivo-](#)  
604 [pluvial streams, where the tail-up flow-connected component accounted for more than 40%](#)  
605 [of the residual variance. This could be due to the distribution of multiple sampling sites along](#)  
606 [the same river segments, as occurred in the eastern section of the basin. However, the](#)  
607 [Euclidean component, which reflects large scale variability across the basin, also accounted](#)  
608 [for more than 35% of the variance in nivo-pluvial streams. This may be due to the fact that](#)  
609 [streams with nivo-pluvial regimes were relatively more widely distributed throughout the](#)  
610 [basin.](#)

611 These findings are in line with a recent study from the US where SSN models were used to  
612 examine variation in fish community traits (Bruckerhoff et al., 2018). However, comparison  
613 across studies is challenging as the effects of spatial autocorrelation in a given model depend  
614 on the response variable and the covariates included, as well as on the spatial relationship of  
615 samples. Therefore, spatial effects may vary substantially across regions, but they are likely  
616 relevant for flow-ecology studies when these are paralleled with flow regime classification in  
617 which sites might be spatially structured (e.g. Bruckerhoff et al., 2019; Snelder & Booker,  
618 2013). Ignoring such spatial dependency could lead to increased Type I error rates (“false  
619 positive”; Legendre & Legendre, 2012), with important implications for the success of *e-*  
620 *flows* design.

621 An additional issue to consider is that, although we selected streams with no evident  
622 alteration of flow regime, the influence of other factors on stream invertebrates was evident.  
623 [The negative effect of agricultural land-use on multiple biotic metrics was evident \(e.g.](#)  
624 [richness, Star\\_ICMi\), especially in the nivo-glacial and nivo-pluvial streams, while water](#)

625 quality had the strongest (positive) influence on the lower gradient pluvial streams (e.g.  
626 increasing diversity, shredders, predators). These results are not surprising and in line with a  
627 recent study that included a larger sample of locations throughout the basin (Larsen et al.,  
628 2019). However, this highlights how defining a baseline flow-ecology relationship under  
629 natural conditions might become increasingly difficult as river catchments are modified  
630 globally (Tickner et al., 2020). In addition, alteration of flow regimes is often accompanied  
631 by changes in water temperature and in-stream habitat structure (e.g. Zolezzi et al., 2011).  
632 Therefore, non-hydrologic factors must be incorporated in *e-flow* frameworks to identify  
633 circumstances that might limit the desired outcome of flow management (Poff, 2018).

634

635 At the management level of *e-flows* setting, the present work represents the first **data-driven**  
636 classification of natural flow regimes in Italy that is paralleled by an ecological assessment.  
637 Previous catchment regionalisation schemes were produced at the national scale (Di Prinzio  
638 et al., 2011), but they focused primarily on estimating streamflow at ungauged sites. Results  
639 demonstrated that flow-ecology relationships can substantially vary among flow regimes,  
640 highlighting the importance of developing *e-flows* tailored to specific eco-hydrologic  
641 contexts. Moreover, although analyses were conducted within a single river basin, and thus  
642 minimized the influence of larger-scale confounding factors, spatial patterns accounted for  
643 most of the variance in the data. The importance of using spatially-explicit approaches to  
644 model empirical data in river networks is increasingly recognised (Frieden et al., 2014; Isaak  
645 et al., 2017; Larsen et al., 2019), and our results further support their application in flow-  
646 ecology research (Bruckerhoff et al., 2019).

647 In conclusion, we addressed three main challenges of flow-ecology research derived from:  
648 i) the limited availability of streamflow time series at sampling sites, ii) the natural variability  
649 of flow regimes and iii) the spatial autocorrelation unique to dendritic river networks. In  
650 doing so we also completed the first two steps of the ELOHA framework (Poff et al., 2010),  
651 **namely developing the hydrological foundation and classifying natural flow regimes across**  
652 **the catchment;** to our best **knowledge, it is the first time that this is applied** to a very  
653 heterogeneous Alpine river catchment.

654 Future developments should address the challenge of incorporating hydrologic variability  
655 when setting environmental flows, and of assessing the ecological effects of specific flow  
656 events or sequence of events without relying on stationary long-term flow records as baseline  
657 reference (Horne et al., 2019; Poff, 2018). The framework presented in this paper could thus  
658 be extended to include future climate scenarios to feed the hydrologic model. Simulated

659 projections of streamflow could then be used to estimate future ecological responses to flow  
660 alteration.

661

662

## 663 **Acknowledgements**

664 This project has received funding from the European Union’s Horizon 2020 research and  
665 innovation programme under the Marie Skłodowska-Curie Grant Agreement No. 748969,  
666 awarded to SL. Further financial support was received by the Italian Ministry of Education,  
667 University and Research (MIUR) under the Departments of Excellence, grant L.232/2016,  
668 and by the Energy oriented Centre of Excellence (EoCoE-II), GA number 824158, funded  
669 within the Horizon 2020 framework of the European Union. Bruno Majone also  
670 acknowledges support by the project "Seasonal Hydrological-Econometric forecasting for  
671 hydropower optimization (SHE)" funded within the Call for projects “Research Südtirol/Alto  
672 Adige” 2019 Autonomous Province of Bozen/Bolzano – South Tyrol. Streamflow data were  
673 provided by the Hydrographic Office of the Autonomous Province of Bolzano  
674 ([www.provincia.bz.it/hydro](http://www.provincia.bz.it/hydro)) and by the Service for Hydraulic Works of the Autonomous  
675 Province of Trento ([www.floods.it](http://www.floods.it)). We are grateful to Jay Ver Hoef for advice on the SSN  
676 models. Comments from three anonymous reviewers greatly improved the quality of the  
677 manuscript.

678 Data supporting this research will be archived in the Dryad repository upon acceptance of the  
679 manuscript and publicly available at: DOI <https://doi.org/10.5061/dryad.vdncjsxt1>

680

681

682

## 683 **References**

684

685 Anderson, M. J. (2017). Permutational Multivariate Analysis of Variance (PERMANOVA).

686 In *Wiley StatsRef: Statistics Reference Online* (pp. 1–15). American Cancer Society.

687 <https://doi.org/10.1002/9781118445112.stat07841>

688 Arthington, A. H., Bhaduri, A., Bunn, S. E., Jackson, S. E., Tharme, R. E., Tickner, D., et al.

689 (2018). The Brisbane Declaration and Global Action Agenda on Environmental Flows

690 (2018). *Frontiers in Environmental Science*, 6.

691 <https://doi.org/10.3389/fenvs.2018.00045>

- 692 Avesani, D., Galletti, A., Piccolroaz, S., Bellin, A., & Majone, B. (2021). A dual-layer MPI  
693 continuous large-scale hydrological model including Human Systems. *Environmental*  
694 *Modelling & Software* (in press).
- 695 Azzellino, A., Canobbio, S., Çervigen, S., Marchesi, V., & Piana, A. (2015). Disentangling  
696 the multiple stressors acting on stream ecosystems to support restoration priorities.  
697 *Water Science & Technology*, 72(2), 293. <https://doi.org/10.2166/wst.2015.177>
- 698 Bellin, A., Majone, B., Cainelli, O., Alberici, D., & Villa, F. (2016). A continuous coupled  
699 hydrological and water resources management model. *Environmental Modelling &*  
700 *Software*, 75, 176–192. <https://doi.org/10.1016/j.envsoft.2015.10.013>
- 701 Belmar, Velasco, J., & Martinez-Capel, F. (2011). Hydrological Classification of Natural  
702 Flow Regimes to Support Environmental Flow Assessments in Intensively Regulated  
703 Mediterranean Rivers, Segura River Basin (Spain). *Environmental Management*,  
704 47(5), 992. <https://doi.org/10.1007/s00267-011-9661-0>
- 705 Beven, K. (2012). *Rainfall-Runoff Modelling: The Primer*. Wiley-Blackwell.
- 706 Booker, D. J., Snelder, T. H., Greenwood, M. J., & Crow, S. K. (2015). Relationships  
707 between invertebrate communities and both hydrological regime and other  
708 environmental factors across New Zealand's rivers. *Ecohydrology*, 8(1), 13–32.  
709 <https://doi.org/10.1002/eco.1481>
- 710 Brighenti, S, Tolotti, M, Bertoldi, W, Wharton, G, Bruno, MC. Rock glaciers and paraglacial  
711 features influence stream invertebrates in a deglaciating Alpine area. *Freshwater*  
712 *Biology*. 2020; 00: 1– 14. <https://doi.org/10.1111/fwb.13658>
- 713 **Brittain, J. E., & Eikeland, T. J. (1988). Invertebrate drift — a review. *Hydrobiologia*, 166(1):**  
714 **77–93. <https://doi.org/10.1007/BF00017485>.**
- 715 Brown, L. E., Hannah, D. M., & Milner, A. M. (2003). Alpine Stream Habitat Classification:  
716 An Alternative Approach Incorporating the Role of Dynamic Water Source  
717 Contributions. *Arctic, Antarctic, and Alpine Research*, 35(3), 313–322.  
718 [https://doi.org/10.1657/1523-0430\(2003\)035\[0313:ASHCAA\]2.0.CO;2](https://doi.org/10.1657/1523-0430(2003)035[0313:ASHCAA]2.0.CO;2)
- 719 Bruckerhoff, L. A., Leasure, D. R., & Magoulick, D. D. (2019). Flow–ecology relationships  
720 are spatially structured and differ among flow regimes. *Journal of Applied Ecology*,  
721 56(2), 398–412. <https://doi.org/10.1111/1365-2664.13297>
- 722 Buchanan, C., Moltz, H. L. N., Haywood, H. C., Palmer, J. B., & Griggs, A. N. (2013). A test  
723 of The Ecological Limits of Hydrologic Alteration (ELOHA) method for determining  
724 environmental flows in the Potomac River basin, U.S.A. *Freshwater Biology*, 58(12),  
725 2632–2647. <https://doi.org/10.1111/fwb.12240>

- 726 Carrara, F., Altermatt, F., Rodriguez-Iturbe, I., & Rinaldo, A. (2012). Dendritic connectivity  
727 controls biodiversity patterns in experimental metacommunities. *Proceedings of the*  
728 *National Academy of Sciences*, *109*(15), 5761–5766.  
729 <https://doi.org/10.1073/pnas.1119651109>
- 730 Chiogna, G., Majone, B., Cano Paoli, K., Diamantini, E., Stella, E., Mallucci, S., et al.  
731 (2016). A review of hydrological and chemical stressors in the Adige catchment and  
732 its ecological status. *Science of The Total Environment*, *540*, 429–443.  
733 <https://doi.org/10.1016/j.scitotenv.2015.06.149>
- 734 Couto, T. B., & Olden, J. D. (2018). Global proliferation of small hydropower plants –  
735 science and policy. *Frontiers in Ecology and the Environment*, *16*(2), 91–100.  
736 <https://doi.org/10.1002/fee.1746>
- 737 De Pauw, N., Gabriels, W., & Goethals, P. L. M. (2006). River Monitoring and Assessment  
738 Methods Based on Macroinvertebrates. In *Biological Monitoring of Rivers* (pp. 111–  
739 134). Wiley-Blackwell. <https://doi.org/10.1002/0470863781.ch7>
- 740 Di Prinzio, M., Castellarin, A., & Toth, E. (2011). Data-driven catchment classification:  
741 application to the pub problem. *Hydrology and Earth System Sciences*, *15*(6), 1921–  
742 1935. <https://doi.org/10.5194/hess-15-1921-2011>
- 743 Diamantini, E., Lutz, S. R., Mallucci, S., Majone, B., Merz, R., & Bellin, A. (2018). Driver  
744 detection of water quality trends in three large European river basins. *Science of The*  
745 *Total Environment*, *612*, 49–62. <https://doi.org/10.1016/j.scitotenv.2017.08.172>
- 746 Doretto, A., Bona, F., Falasco, E., Morandini, D., Piano, E., & Fenoglio, S. (2020). Stay with  
747 the flow: How macroinvertebrate communities recover during the rewetting phase in  
748 Alpine streams affected by an exceptional drought. *River Research and Applications*,  
749 *36*(1), 91–101. <https://doi.org/10.1002/rra.3563>
- 750 European Commission. (2000). Directive 2000/60/EC of 20 December 2000 of the European  
751 Union and of the Council establishing a framework for community action in the field  
752 of water policy. Official Journal of the European Communities.
- 753 Fornaroli, R., Cabrini, R., Sartori, L., Marazzi, F., Vrincevic, D., Mezzanotte, V., et al. (2015).  
754 Predicting the constraint effect of environmental characteristics on macroinvertebrate  
755 density and diversity using quantile regression mixed model. *Hydrobiologia*, *742*(1),  
756 153–167. <https://doi.org/10.1007/s10750-014-1974-6>
- 757 Friberg, N. (2014). Impacts and indicators of change in lotic ecosystems. *Wiley*  
758 *Interdisciplinary Reviews: Water*, *1*(6), 513–531. <https://doi.org/10.1002/wat2.1040>
- 759 Frieden, J. C., Peterson, E. E., Angus Webb, J., & Negus, P. M. (2014). Improving the

760 predictive power of spatial statistical models of stream macroinvertebrates using  
761 weighted autocovariance functions. *Environmental Modelling & Software*, 60, 320–  
762 330. <https://doi.org/10.1016/j.envsoft.2014.06.019>

763 Garreta, V., Monestiez, P., & Ver Hoef, J. M. (2009). Spatial modelling and prediction on  
764 river networks: up model, down model or hybrid? *Environmetrics*, 21, 439-456  
765 <https://doi.org/10.1002/env.995>

766 Goovaerts, P. (1997). *Geostatistics for Natural Resources Evaluation*. Oxford University  
767 Press.

768 Green, P. A., Vörösmarty, C. J., Harrison, I., Farrell, T., Sáenz, L., & Fekete, B. M. (2015).  
769 Freshwater ecosystem services supporting humans: Pivoting from water crisis to  
770 water solutions. *Global Environmental Change*, 34, 108–118.  
771 <https://doi.org/10.1016/j.gloenvcha.2015.06.007>

772 Grill, G., Lehner, B., Thieme, M., Geenen, B., Tickner, D., Antonelli, F., et al. (2019).  
773 Mapping the world's free-flowing rivers. *Nature*, 569(7755), 215–221.  
774 <https://doi.org/10.1038/s41586-019-1111-9>

775 Heino, J., Schmera, D., & Erős, T. (2013). A macroecological perspective of trait patterns in  
776 stream communities. *Freshwater Biology*, 58(8), 1539–1555.  
777 <https://doi.org/10.1111/fwb.12164>

778 Heisterman, M. & Kneis, D. (2011). Benchmarking quantitative precipitation estimation by  
779 conceptual rainfall-runoff modeling. *Water Resources Research*, 47(6).  
780 <https://doi.org/10.1029/2010WR009153>.

781 Horne, A. C., Nathan, R., Poff, N. L., Bond, N. R., Webb, J. A., Wang, J., & John, A. (2019).  
782 Modeling Flow-Ecology Responses in the Anthropocene: Challenges for Sustainable  
783 Riverine Management. *BioScience*, 69(10), 789–799.  
784 <https://doi.org/10.1093/biosci/biz087>

785 Ilg, C., Castella, E., Lods-Crozet, B., & Marmorier, P. (2001). Invertebrate drift and physico-  
786 chemical variables in the tributaries of the Mutt, a Swiss glacial stream. *Arch.*  
787 *Hydrobiol.*, 151, 335–352. <https://doi.org/10.1127/archiv-hydrobiol/151/2001/335>

788 Isaak, D. J., Peterson, E. E., Ver Hoef, J. M., Wenger, S. J., Falke, J. A., Torgersen, C. E., et  
789 al. (2014). Applications of spatial statistical network models to stream data: Spatial  
790 statistical network models for stream data. *Wiley Interdisciplinary Reviews: Water*,  
791 1(3), 277–294. <https://doi.org/10.1002/wat2.1023>

792 Isaak, D. J., Ver Hoef, J. M., Peterson, E. E., Horan, D. L., & Nagel, D. E. (2017). Scalable  
793 population estimates using spatial-stream-network (SSN) models, fish density

794 surveys, and national geospatial database frameworks for streams. *Canadian Journal*  
795 *of Fisheries and Aquatic Sciences*, 74(2), 147–156. [https://doi.org/10.1139/cjfas-](https://doi.org/10.1139/cjfas-2016-0247)  
796 2016-0247

797 Jost, L. (2006). Entropy and diversity. *Oikos*, 113(2), 363–375.  
798 <https://doi.org/10.1111/j.2006.0030-1299.14714.x>

799 Kennedy, J., & Eberhart, R. (1995). Particle swarm optimization. In *Proceedings of ICNN'95*.  
800 Kennedy, T.A., Muehlbauer, J.D., Yackulic, C.B., Lytle, D.A., Miller, S.W., Dibble, K.L.,  
801 Kortenhoeven, E.W., Metcalfe, A.N. & Baxter, C.V. (2016). Flow management for  
802 hydropower extirpates aquatic insects, undermining river food webs. *BioScience*, 66,  
803 561-575. <https://doi.org/10.1093/biosci/biw059>

804 Kennen, J. G., Riva - Murray, K., & Beaulieu, K. M. (2010). Determining hydrologic factors  
805 that influence stream macroinvertebrate assemblages in the northeastern US.  
806 *Ecohydrology*, 3(1), 88–106. <https://doi.org/10.1002/eco.99>

807 Kiesel, J., Kakouei, K., Guse, B., Fohrer, N., & Jähnig, S. C. (2020). When is a hydrological  
808 model sufficiently calibrated to depict flow preferences of riverine species?  
809 *Ecohydrology*, 13(3), e2193. <https://doi.org/10.1002/eco.2193>

810 Konrad, C. P., Brasher, A. M. D., & May, J. T. (2008). Assessing streamflow characteristics  
811 as limiting factors on benthic invertebrate assemblages in streams across the western  
812 United States. *Freshwater Biology*, 53(10), 1983–1998.  
813 <https://doi.org/10.1111/j.1365-2427.2008.02024.x>

814 Laiti, L., Mallucci, S., Piccolroaz, S., Bellin, A., Zardi, D., Fiori, A., et al. (2018). Testing the  
815 Hydrological Coherence of High-Resolution Gridded Precipitation and Temperature  
816 Data Sets. *Water Resources Research*, 54(3), 1999–2016.  
817 <https://doi.org/10.1002/2017WR021633>

818 Larsen, S., Bruno, M. C., Vaughan, I. P., & Zolezzi, G. (2019). Testing the River Continuum  
819 Concept with geostatistical stream-network models. *Ecological Complexity*, 39,  
820 100773. <https://doi.org/10.1016/j.ecocom.2019.100773>

821 Larsen, S., Bruno, M. C., & Zolezzi, G. (2019). WFD ecological status indicator shows poor  
822 correlation with flow parameters in a large Alpine catchment. *Ecological Indicators*,  
823 98, 704–711. <https://doi.org/10.1016/j.ecolind.2018.11.047>

824 Legendre, P., & Legendre, L. (2012). *Numerical Ecology, Volume 24 - 3rd Edition*. Elsevier.  
825 Retrieved from [https://www.elsevier.com/books/numerical-ecology/legendre/978-0-](https://www.elsevier.com/books/numerical-ecology/legendre/978-0-444-53868-0)  
826 444-53868-0

- 827 Lutz, S. R., Mallucci, S., Diamantini, E., Majone, B., Bellin, A., & Merz, R. (2016).  
828 Hydroclimatic and water quality trends across three Mediterranean river basins.  
829 *Science of The Total Environment*, 571, 1392–1406.  
830 <https://doi.org/10.1016/j.scitotenv.2016.07.102>
- 831 Majone, B., Bertagnoli, A., & Bellin, A. (2010). A non-linear runoff generation model in  
832 small Alpine catchments. *Journal of Hydrology*, 385(1), 300–312.  
833 <https://doi.org/10.1016/j.jhydrol.2010.02.033>
- 834 Majone, B., Villa, F., Deidda, R., & Bellin, A. (2016). Impact of climate change and water  
835 use policies on hydropower potential in the south-eastern Alpine region. *Science of*  
836 *The Total Environment*, 543, 965–980.  
837 <https://doi.org/10.1016/j.scitotenv.2015.05.009>
- 838 Mallucci, S., Majone, B., & Bellin, A. (2019). Detection and attribution of hydrological  
839 changes in a large Alpine river basin. *Journal of Hydrology*, 575, 1214–1229.  
840 <https://doi.org/10.1016/j.jhydrol.2019.06.020>
- 841 Mazor, R. D., May, J. T., Sengupta, A., McCune, K. S., Bledsoe, B. P., & Stein, E. D. (2018).  
842 Tools for managing hydrologic alteration on a regional scale: Setting targets to protect  
843 stream health. *Freshwater Biology*. <https://doi.org/10.1111/fwb.13062>
- 844 McGuire, K. J., Torgersen, C. E., Likens, G. E., Buso, D. C., Lowe, W. H., & Bailey, S. W.  
845 (2014). Network analysis reveals multiscale controls on streamwater chemistry.  
846 *Proceedings of the National Academy of Sciences*, 111(19), 7030–7035.  
847 <https://doi.org/10.1073/pnas.1404820111>
- 848 McManamay, R.A., Orth, D.J., Dolloff, C.A. & Frimpong, E.A. (2012). A Regionla  
849 classification of unregulated stream flows: spatial resolution and hierarchical  
850 frameworks. *River Research and Applications*, 28, 1019-1033.
- 851 Merigoux, S., & Doledec, S. (2004). Hydraulic requirements of stream communities: a case  
852 study on invertebrates. *Freshwater Biology*, 49(5), 600–613.  
853 <https://doi.org/10.1111/j.1365-2427.2004.01214.x>
- 854 Michel, C., Andréassian, V., & Perrin, C. (2005). Soil Conservation Service Curve Number  
855 method: How to mend a wrong soil moisture accounting procedure? *Water Resources*  
856 *Research*, 41(2). <https://doi.org/10.1029/2004WR003191>
- 857 Mims, M. C., & Olden, J. D. (2012). Life history theory predicts fish assemblage response to  
858 hydrologic regimes. *Ecology*, 93(1), 35–45. <https://doi.org/10.1890/11-0370.1>
- 859 Naman, S. M., Rosenfeld J. S., & Richardson, J. S. (2016). Causes and consequences of  
860 invertebrate drift in running waters: from individuals to populations and trophic

861 fluxes. *Canadian Journal of Fisheries and Aquatic Sciences*, 73, 1292–1305.  
862 <https://doi.org/10.1139/cjfas-2015-0363>

863 Navarro-Ortega, A., Acuña, V., Bellin, A., Burek, P., Cassiani, G., Choukr-Allah, R., et al.  
864 (2015). Managing the effects of multiple stressors on aquatic ecosystems under water  
865 scarcity. The GLOBAQUA project. *Science of The Total Environment*, 503–504, 3–9.  
866 <https://doi.org/10.1016/j.scitotenv.2014.06.081>

867 Olden, J. D., & Poff, N. L. (2003). Redundancy and the choice of hydrologic indices for  
868 characterizing streamflow regimes. *River Research and Applications*, 19(2), 101–121.  
869 <https://doi.org/10.1002/rra.700>

870 Patrick, C. J., & Yuan, L. L. (2017a). Modeled hydrologic metrics show links between  
871 hydrology and the functional composition of stream assemblages. *Ecological*  
872 *Applications*, 27(5), 1605–1617. <https://doi.org/10.1002/eap.1554>

873 Patrick, C. J., & Yuan, L. L. (2017b). Modeled hydrologic metrics show links between  
874 hydrology and the functional composition of stream assemblages. *Ecological*  
875 *Applications*, 27(5), 1605–1617. <https://doi.org/10.1002/eap.1554>

876 Peterson, E. E., & Hoef, J. M. V. (2014). STARS: An ArcGIS Toolset Used to Calculate the  
877 Spatial Information Needed to Fit Spatial Statistical Models to Stream Network Data.  
878 *Journal of Statistical Software*, 56(2). <https://doi.org/10.18637/jss.v056.i02>

879 Peterson, E. E., Ver Hoef, J. M., Isaak, D. J., Falke, J. A., Fortin, M.-J., Jordan, C. E., et al.  
880 (2013). Modelling dendritic ecological networks in space: an integrated network  
881 perspective. *Ecology Letters*, 16(5), 707–719. <https://doi.org/10.1111/ele.12084>

882 Piccolroaz, S., Lazzaro, M. D., Zarlenga, A., Majone, B., Bellin, A., & Fiori, A. (2016).  
883 HYPERstream: a multi-scale framework for streamflow routing in large-scale  
884 hydrological model. *Hydrology and Earth System Sciences*, 20(5), 2047–2061.  
885 <https://doi.org/10.5194/hess-20-2047-2016>

886 Poff. (2018). Beyond the natural flow regime? Broadening the hydro-ecological foundation to  
887 meet environmental flows challenges in a non-stationary world. *Freshwater Biology*,  
888 63(8), 1011–1021. <https://doi.org/10.1111/fwb.13038>

889 Poff, Richter, B. D., Arthington, A. H., Bunn, S. E., Naiman, R. J., Kendy, E., et al. (2010).  
890 The ecological limits of hydrologic alteration (ELOHA): a new framework for  
891 developing regional environmental flow standards: Ecological limits of hydrologic  
892 alteration. *Freshwater Biology*, 55(1), 147–170. [https://doi.org/10.1111/j.1365-](https://doi.org/10.1111/j.1365-2427.2009.02204.x)  
893 [2427.2009.02204.x](https://doi.org/10.1111/j.1365-2427.2009.02204.x)

894 Poff, N. L., Allan, J. D., Bain, M. B., Karr, J. R., Prestegard, K. L., Richter, B. D., et al.

895 (1997). The Natural Flow Regime. *BioScience*, 47(11), 769–784.  
896 <https://doi.org/10.2307/1313099>

897 Poff, N. L., Olden, J. D., Vieira, N. K. M., Finn, D. S., Simmons, M. P., & Kondratieff, B. C.  
898 (2006). Functional trait niches of North American lotic insects: traits-based ecological  
899 applications in light of phylogenetic relationships. *Journal of the North American*  
900 *Benthological Society*, 25(4), 730–755. [https://doi.org/10.1899/0887-](https://doi.org/10.1899/0887-3593(2006)025[0730:FTNONA]2.0.CO;2)  
901 [3593\(2006\)025\[0730:FTNONA\]2.0.CO;2](https://doi.org/10.1899/0887-3593(2006)025[0730:FTNONA]2.0.CO;2)

902 Quadroni, S., Crosa, G., Gentili, G., & Espa, P. (2017). Response of stream benthic  
903 macroinvertebrates to current water management in Alpine catchments massively  
904 developed for hydropower. *Science of The Total Environment*, 609, 484–496.  
905 <https://doi.org/10.1016/j.scitotenv.2017.07.099>

906 R Core Team. (2019). *R: A language and environment for statistical computing*. Vienna.

907 Richter, B., Baumgartner, J., Wigington, R., & Braun, D. (1997). How much water does a  
908 river need? *Freshwater Biology*, 37(1), 231–249. [https://doi.org/10.1046/j.1365-](https://doi.org/10.1046/j.1365-2427.1997.00153.x)  
909 [2427.1997.00153.x](https://doi.org/10.1046/j.1365-2427.1997.00153.x)

910 Rinaldo, A., Marani, A., & Rigon, R. (1991). Geomorphological dispersion. *Water Resources*  
911 *Research*, 27(4), 513–525. <https://doi.org/10.1029/90WR02501>

912 **Robinson, C. T., Tockner, K. & Burgherr, P. (2004). Drift benthos relationships in the**  
913 **seasonal colonization dynamics of alpine streams. *Arch. Hydrobiol.*, 160(4), 447–470.**  
914 **<https://doi.org/10.1127/0003-9136/2004/0160-0447>**

915 Rosenfeld, J. S. (2017). Developing flow–ecology relationships: Implications of nonlinear  
916 biological responses for water management. *Freshwater Biology*, 62(8), 1305–1324.  
917 <https://doi.org/10.1111/fwb.12948>

918 Schmidt-Kloiber, A., & Hering, D. (2015). [www.freshwaterecology.info](http://www.freshwaterecology.info) – An online tool that  
919 unifies, standardises and codifies more than 20,000 European freshwater organisms  
920 and their ecological preferences. *Ecological Indicators*, 53, 271–282.  
921 <https://doi.org/10.1016/j.ecolind.2015.02.007>

922 Shumilova, O., Tockner, K., Thieme, M., Koska, A., & Zarfl, C. (2018). Global Water  
923 Transfer Megaprojects: A Potential Solution for the Water-Food-Energy Nexus?  
924 *Frontiers in Environmental Science*, 6. <https://doi.org/10.3389/fenvs.2018.00150>

925 Skøien, J. O., Merz, R., & Blöschl, G. (2006). Top-kriging - geostatistics on stream networks.  
926 *Hydrology and Earth System Sciences*, 10(2), 277–287. [https://doi.org/10.5194/hess-](https://doi.org/10.5194/hess-10-277-2006)  
927 [10-277-2006](https://doi.org/10.5194/hess-10-277-2006)

928 Snelder, T. H., & Booker, D. J. (2013). Natural Flow Regime Classifications Are Sensitive to

929 Definition Procedures. *River Research and Applications*, 29(7), 822–838.  
930 <https://doi.org/10.1002/rra.2581>

931 Strayer, D. L., & Dudgeon, D. (2010). Freshwater biodiversity conservation: recent progress  
932 and future challenges. *Journal of the North American Benthological Society*, 29(1),  
933 344–358. <https://doi.org/10.1899/08-171.1>

934 Tickner, D., Opperman, J. J., Abell, R., Acreman, M., Arthington, A. H., Bunn, S. E., et al.  
935 (2020). Bending the Curve of Global Freshwater Biodiversity Loss: An Emergency  
936 Recovery Plan. *BioScience*, 70(4), 330–342. <https://doi.org/10.1093/biosci/biaa002>

937 Tonkin, J. D., Poff, N. L., Bond, N. R., Horne, A., Merritt, D. M., Reynolds, L. V., et al.  
938 (2019). Prepare river ecosystems for an uncertain future. *Nature*, 570(7761), 301–303.  
939 <https://doi.org/10.1038/d41586-019-01877-1>

940 Ver Hoef, J. M., & Peterson, E. E. (2010). A Moving Average Approach for Spatial  
941 Statistical Models of Stream Networks. *Journal of the American Statistical*  
942 *Association*, 105(489), 6–18. <https://doi.org/10.1198/jasa.2009.ap08248>

943 Ver Hoef, J. M., Peterson, E. E., Clifford, D., & Shah, R. (2014). SSN : An R Package for  
944 Spatial Statistical Modeling on Stream Networks. *Journal of Statistical Software*,  
945 56(3). <https://doi.org/10.18637/jss.v056.i03>

946 Vigiak, O., Lutz, S., Mentzafou, A., Chiogna, G., Tuo, Y., Majone, B., et al. (2018).  
947 Uncertainty of modelled flow regime for flow-ecological assessment in Southern  
948 Europe. *Science of The Total Environment*, 615, 1028–1047.  
949 <https://doi.org/10.1016/j.scitotenv.2017.09.295>

950 Warton, D. I., & Hui, F. K. C. (2011). The arcsine is asinine: the analysis of proportions in  
951 ecology. *Ecology*, 92(1), 3–10. <https://doi.org/10.1890/10-0340.1>

952 Zarfl, C., Lumsdon, A. E., Berlekamp, J., Tydecks, L., & Tockner, K. (2015). A global boom  
953 in hydropower dam construction. *Aquatic Sciences*, 77(1), 161–170.  
954 <https://doi.org/10.1007/s00027-014-0377-0>

955 Zimmerman, D. L., & Ver Hoef, J. M. (2017). The Torgegram for Fluvial Variography:  
956 Characterizing Spatial Dependence on Stream Networks. *Journal of Computational*  
957 *and Graphical Statistics*, 26(2), 253–264.  
958 <https://doi.org/10.1080/10618600.2016.1247006>

959 Zolezzi, G., Bellin, A., Bruno, M. C., Maiolini, B., & Siviglia, A. (2009). Assessing  
960 hydrological alterations at multiple temporal scales: Adige River, Italy. *Water*  
961 *Resources Research*, 45(12). <https://doi.org/10.1029/2008WR007266>

962

963

964 **Tables**

965

966

967 **Table 1-** List of the IHA flow metrics computed from the 23 years simulated streamflow  
968 time series. Metrics in bold were selected for the examination of flow-ecology relationship in  
969 the SSN models.

970

971

972

973

Flow component	IHA flow metric name	Description
<i>1 - Magnitude of monthly flow conditions (12 parameters)</i>	January, February, March, April, May June, July, August, September, October, November, December	Mean flow for January, ..., December
<i>2 - Magnitude and duration of extreme conditions (11 parameters)</i>	1, 3, 7, 30, 90 Day Min	Minimum flow, 1, 3, 7, 30, 90 day mean
	1, 3, 7, 30, 90 Day Max	Maximum flow, 1, 3, 7, 30, 90 day mean
	Base index	7 days minimum / mean flow
<i>3 - Timing of extreme flow conditions (2 parameters)</i>	min Julian	Mean Julian data of annual 1-day maximum
	max Julian	Mean Julian data of annual 1-day minimum
<i>4 - Frequency and duration of high and low pulses (4 parameters)</i>	Low pulse number	Number of flow events below 25th percentile
	High pulse number	Number of flow events above 75th percentile
	Low pulse length	Number of days below 25th percentile
	High pulse length	Number of days above 75th percentile
<i>5 - Rate of change and variation (5 parameters)</i>	Rise rate	Median of all positive differences between consecutive values
	Fall rate	Median of all negative differences between consecutive values
	Reversals	Number of times flow period switches from rising to falling and vice-versa
	y.CV	Average annual coefficient of variation (SD/mean)
	m.CV	Average monthly coefficient of variation (SD/mean)

974

975

976

977

978

979

## 980 **Figures captions**

981

982

983 **Figure 1** - Map of the Adige River network (northeast Italy) showing the locations of the 100  
984 biological monitoring sites for which 25 years of natural streamflow time series were  
985 simulated. Colours define the distribution of the three identified flow regime classes (see  
986 Sect. 2.4). Location of the gauging stations providing observed streamflow series are also  
987 shown, including those used for calibration (c) and validation (d) of the hydrological model.

988

989

990 **Figure 2** - Dendrogram of the study reaches based on flexible beta-clustering of the first two  
991 weighted Principal Components (explaining 92% of variation) of the MAD-normalised  
992 monthly hydrography (expressed as proportion of mean annual discharge). Lower panels  
993 show the mean across sites ( $\pm$  SD) of MAD-normalised hydrographs for each identified  
994 streamflow regime.

995

996

997 **Figure 3-** Boxplot of selected environmental descriptors for each identified streamflow  
998 regime. The following boxplot representation is adopted: horizontal line for median; box for  
999 the inter-quartile range; whiskers for 1.5 times the inter-quartile range; dots for outliers. The  
1000 LIMeco index and the percentage of local agricultural land-use (Agr.landuse) were included  
1001 as covariates in the SSN models.

1002

1003

1004 **Figure 4** - Biplot of the PCA based on 34 IHA flow metrics (direction and loading indicated  
1005 by the blue arrows) derived from the 23 years streamflow series for the 100 investigated  
1006 study sites. The sites are grouped according to the streamflow regime previously determined  
1007 by the flexible beta-clustering approach.

1008

1009

1010

1011

1012 **Figure 5** – Heatmap showing the standardized SSN coefficients ( $\beta$ ) of the covariates included  
1013 in the most supported models for each biotic metric in the three flow regimes, according to  
1014 the RMSPE. 'NS' indicates a non-significant predictor ( $p > 0.05$ ).

1015

1016

1017 **Figure 6** – Scatterplot of selected flow-ecology relationships within each flow regime.  
1018 Continuous and dashed fit lines respectively indicate significant and non-significant  
1019 relationships according to the SSN models. Grey dashed line indicates the overall relationship  
1020 observed combining all three flow regimes.

1021

1022

1023 **Figure 7** – Proportion of variance of each biotic metric explained by the covariates (i.e. flow  
1024 metrics, water quality and local land-use) and by the spatial components modelled with tail-  
1025 up, tail-down and Euclidean autocovariance functions across the three flow regimes. The  
1026 nugget represents the residual variance.

1027

1028

1029

1030

1031

1032

1033

Figure 1.

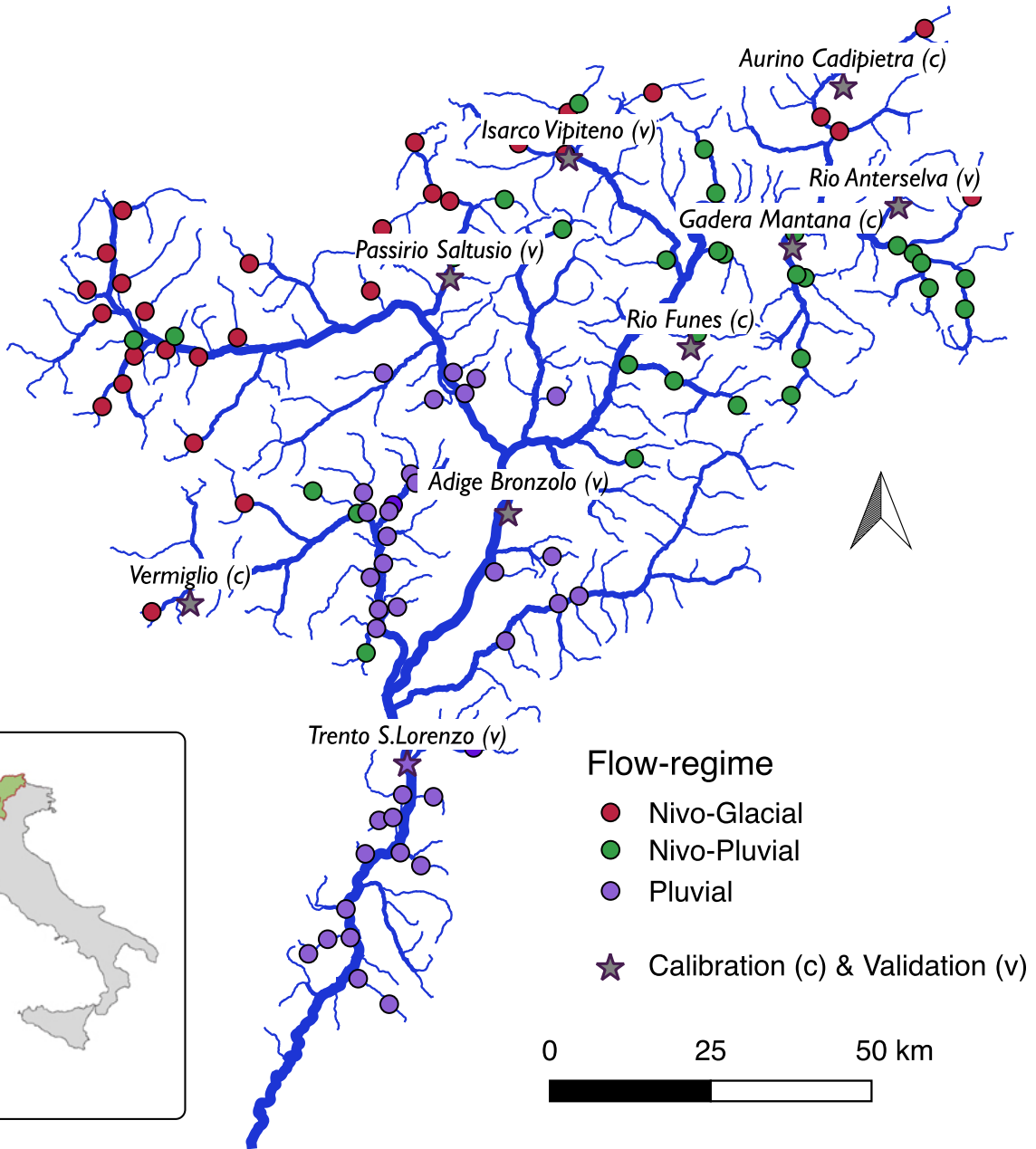
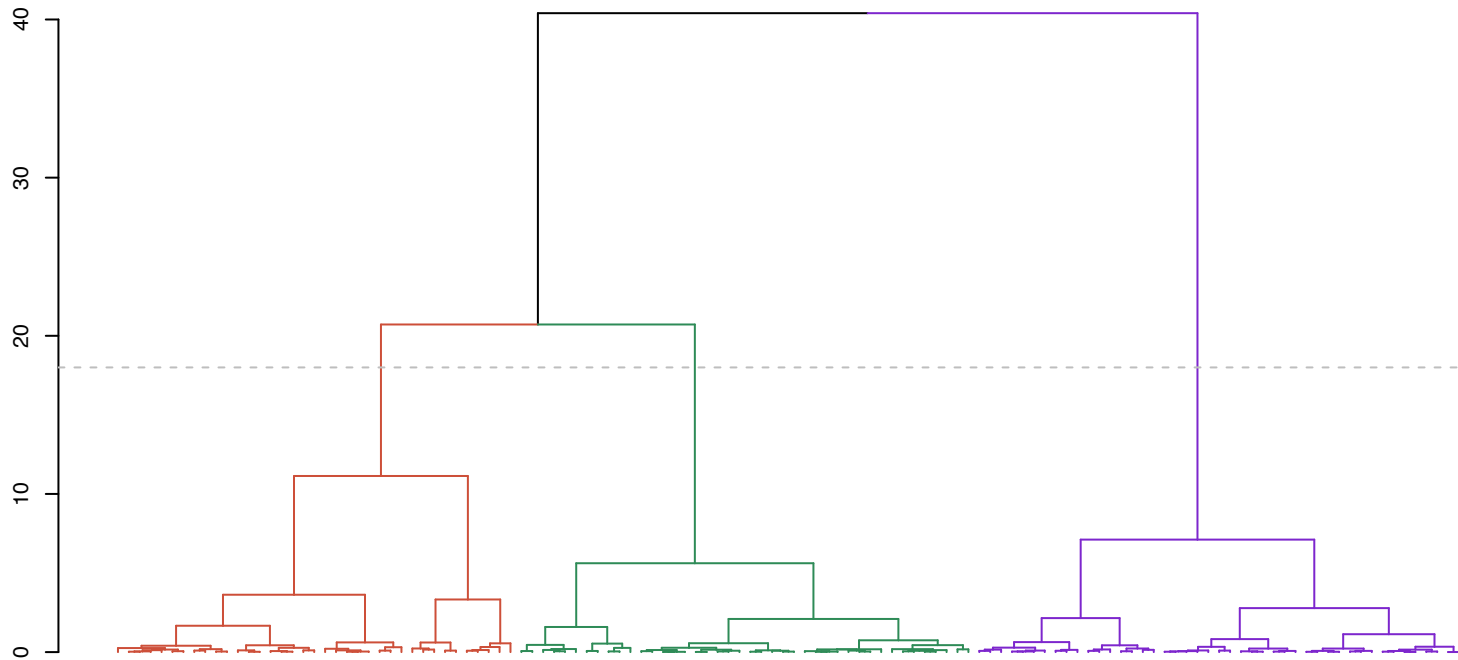
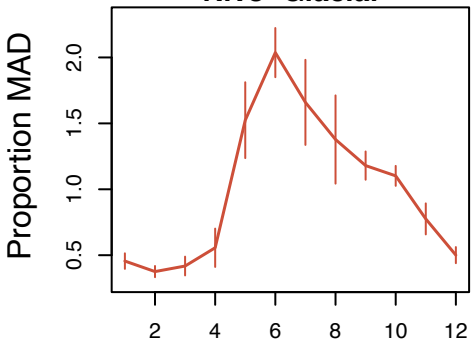


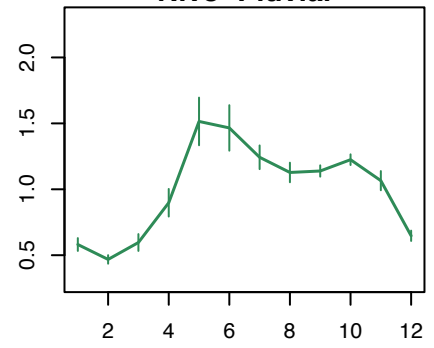
Figure 2.



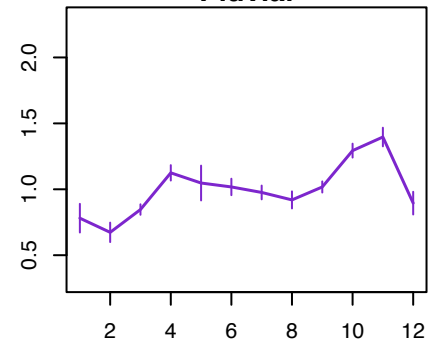
**Nivo-Glacial**



**Nivo-Pluvial**



**Pluvial**

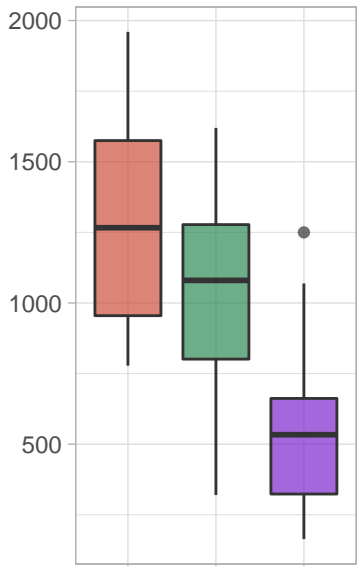


Month

Proportion MAD

Figure 3.

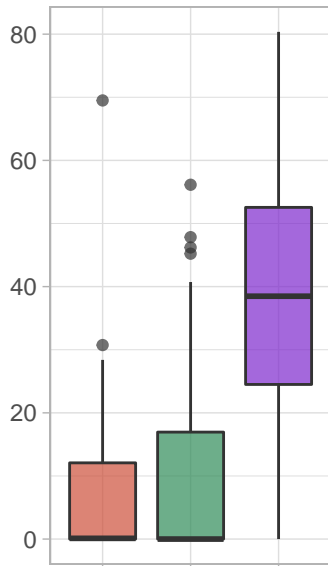
Altitude



LIMeco



Agr.landuse (%)



Flow regime

- Nivo-Glacial
- Nivo-Pluvial
- Pluvial

Figure 4.

# PCA IHA metrics

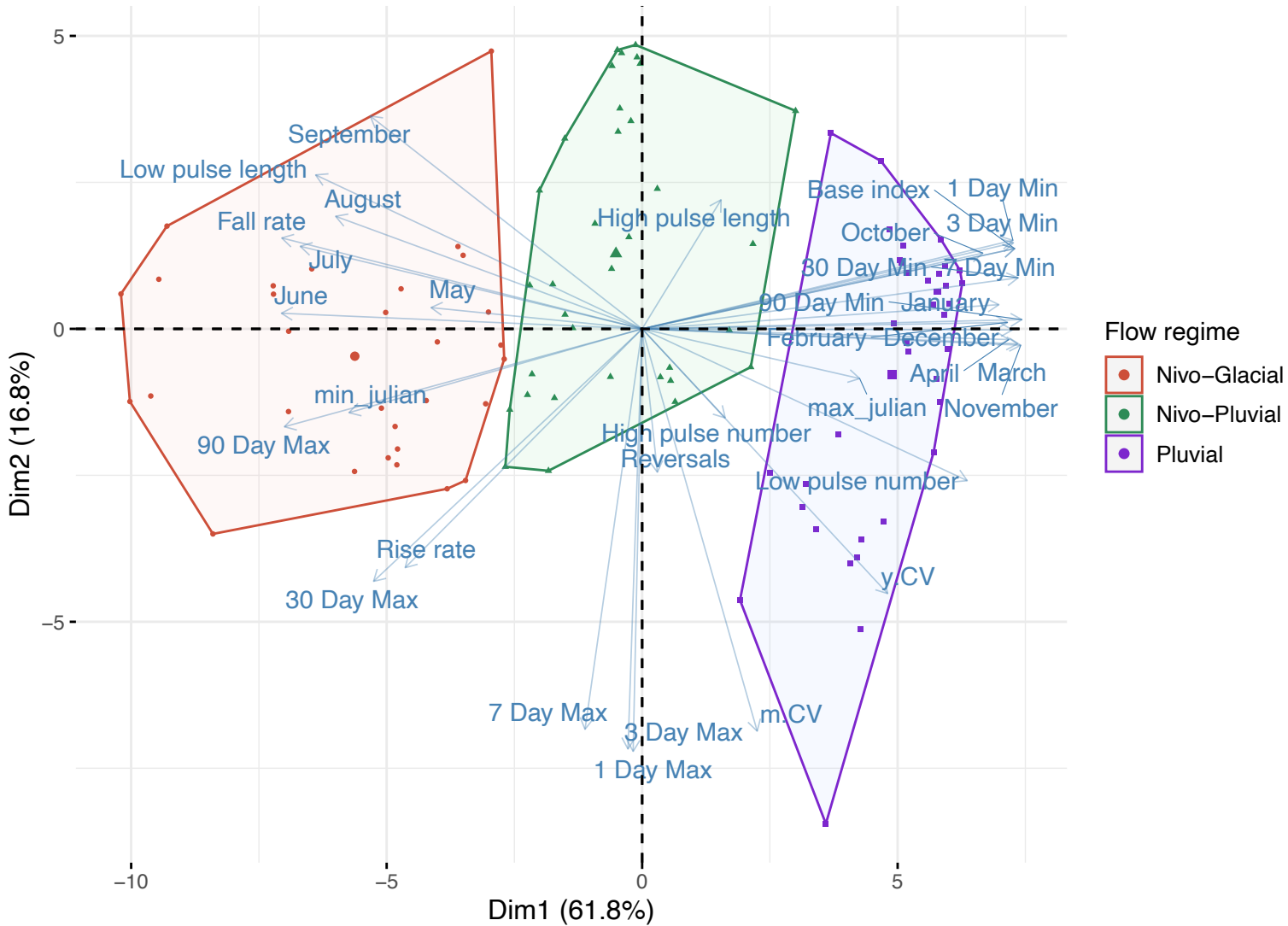
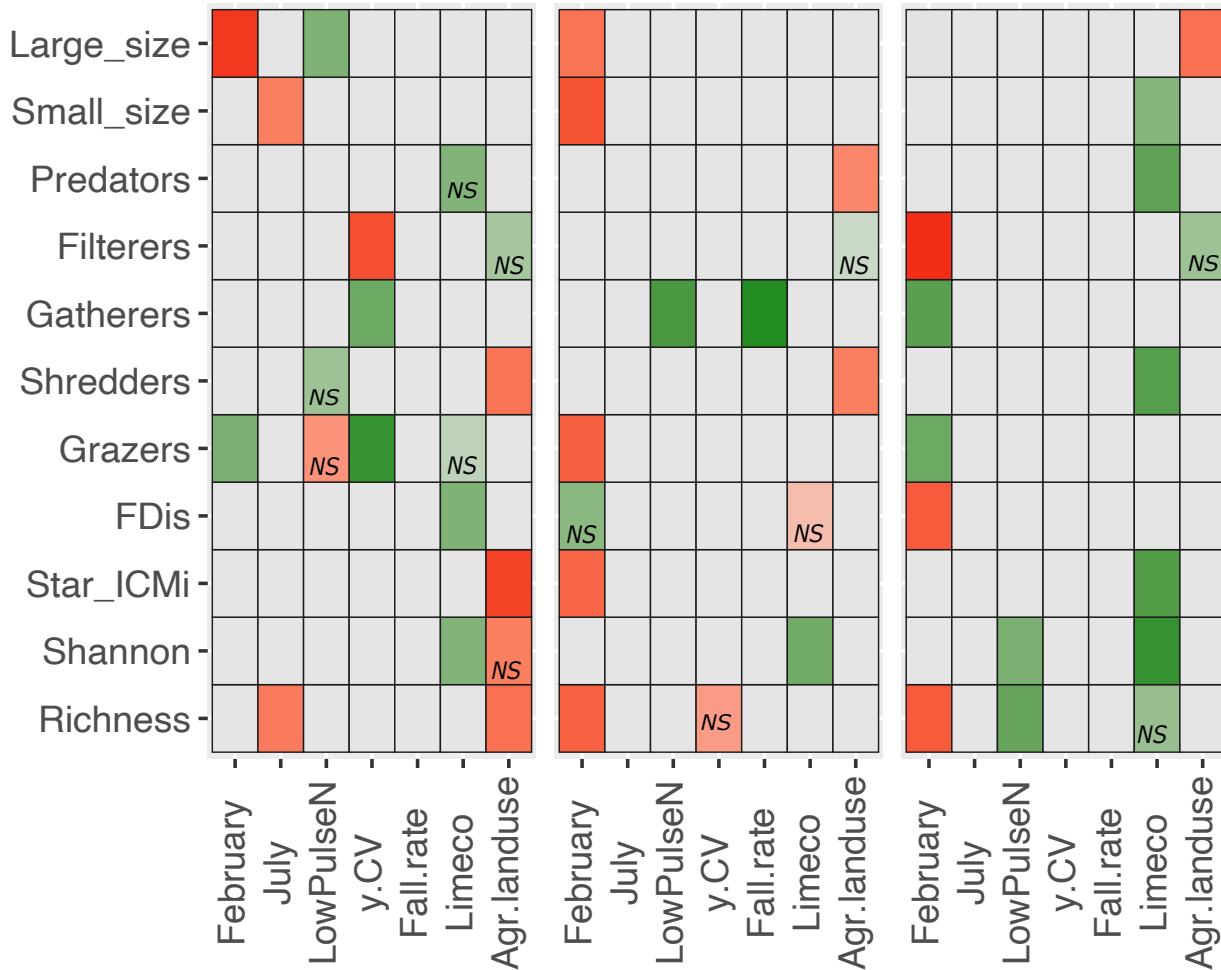


Figure 5.

## Nivo-Glacial

## Nivo-Pluvial

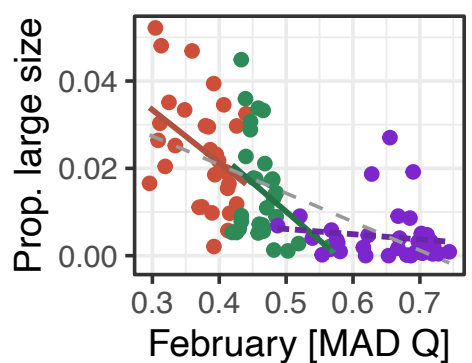
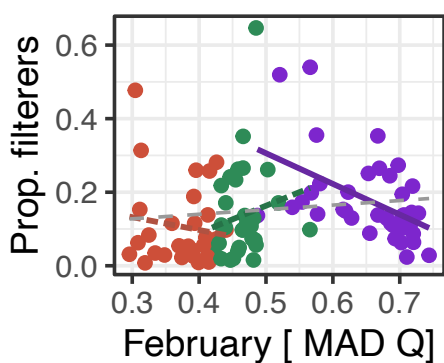
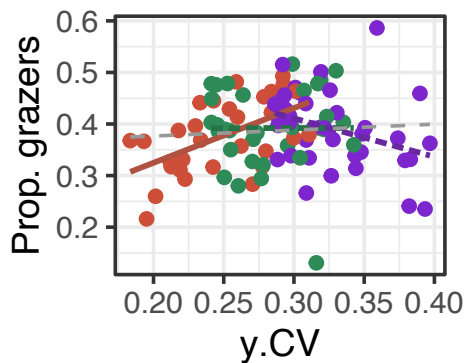
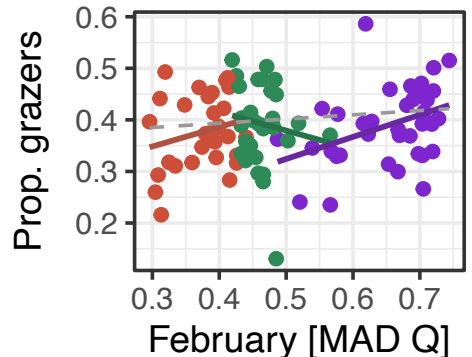
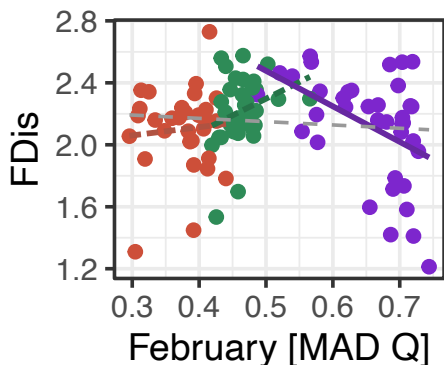
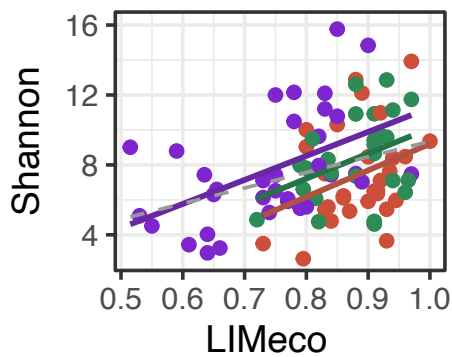
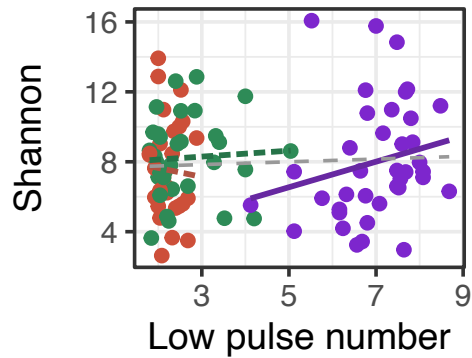
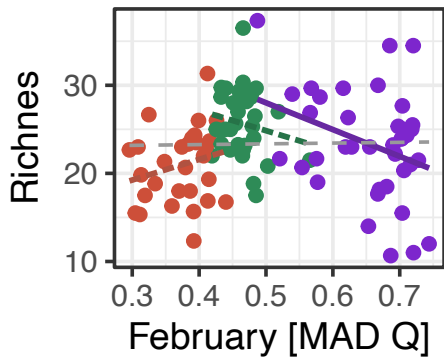
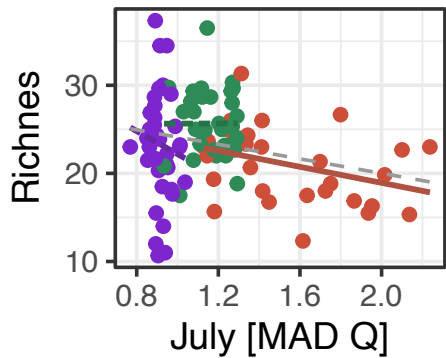
## Pluvial



SSN  $\beta$



Figure 6.



Flow regime

- Nivo-Glacial
- Nivo-Pluvial
- Pluvial

Figure 7.

